Nambu et al. Radiation Oncology 2011, 6:137
http://www.ro-journal.com/content/6/1/137

RADIATION ONCOLOGY

RESEARCH Open Access

Rib fracture after stereotactic radiotherapy on follow-up thin-section computed tomography in 177 primary lung cancer patients

Atsushi Nambu[1*], Hiroshi Onishi[1], Shinichi Aoki[1], Tsuyota Koshiishi[1], Kengo Kuriyama[1], Takafumi Komiyama[2], Kan Marino[3], Masayuki Araya[1], Ryo Saito[1], Lichto Tominaga[1], Yoshiyasu Maehata[1], Eiichi Sawada[1] and Tsutomu Araki[1]

Abstract

Background: Chest wall injury after stereotactic radiotherapy (SRT) for primary lung cancer has recently been reported. However, its detailed imaging findings are not clarified. So this study aimed to fully characterize the findings on computed tomography (CT), appearance time and frequency of chest wall injury after stereotactic radiotherapy (SRT) for primary lung cancer

Materials and methods: A total of 177 patients who had undergone SRT were prospectively evaluated for periodical follow-up thin-section CT with special attention to chest wall injury. The time at which CT findings of chest wall injury appeared was assessed. Related clinical symptoms were also evaluated.

Results: Rib fracture was identified on follow-up CT in 41 patients (23.2%). Rib fractures appeared at a mean of 21.2 months after the completion of SRT (range, 4 -58 months). Chest wall edema, thinning of the cortex and osteosclerosis were findings frequently associated with, and tending to precede rib fractures. No patients with rib fracture showed tumors > 16 mm from the adjacent chest wall. Chest wall pain was seen in 18 of 177 patients (10.2%), of whom 14 patients developed rib fracture. No patients complained of Grade 3 or more symptoms.

Conclusion: Rib fracture is frequently seen after SRT for lung cancer on CT, and is often associated with chest wall edema, thinning of the cortex and osteosclerosis. However, related chest wall pain is less frequent and is generally mild if present.

Keywords: stereotactic radiotherapy, lung cancer, rib fracture, thin-section CT

Background

Stereotactic radiotherapy (SRT) for primary lung cancer has recently attracted attention because of its promising treatment effects [1-10]. A recent report demonstrated that SRT achieved a good survival rate for patients with non-small cell lung carcinoma, comparable to those of surgery [10]. SRT has now been applied not only to medically inoperable patients but also to operable ones. In the near future, SRT might become an alternative treatment to surgery for stage I non-small lung carcinoma.

One major concern that must always been taken into consideration when selecting treatment methods is treatment sequelae. SRT is generally considered a safe treatment, with fewer complications than surgery. However, several studies have reported complications in SRT, such as radiation pneumonitis [11,12] and chest wall injury, including rib fracture [5-7,13-16]. Frequencies of rib fracture after SRT have already been reported in several investigations. However, detailed CT findings of chest wall injury have yet to be clarified.

The present study therefore aimed to fully characterize detailed CT findings of chest wall injury after SRT for primary lung cancer using thin-section CT.

* Correspondence: nambu-a@gray.plala.or.jp
[1]Department of Radiology, University of Yamanashi, Chuo City, Japan
Full list of author information is available at the end of the article

Methods

The institutional review board approved all study protocols. Written informed consent was obtained from all patients prior to participation in this study.

Patients

Between November 2001 and April 2009, a total of 210 patients with primary non-small cell lung carcinoma underwent SRT in our institution. Of these patients, 177 patients agreed to participate in this prospective study. Patient characteristics are summarized in Table 1.

Methods of radiotherapy

SRT was performed using noncoplanar 10 dynamic arcs. A total dose of 48-70Gy at the isocenter was administered in 4-10 fractions, and approximately 80% isodose line of prescribed dose covered planning target volume (PTV) using a 6 MV X-ray, comprising three different methods, namely 48Gy/4fractions, 60Gy/10fractions, and 70Gy/10fractions, (Table 1). We essentially used 60Gy/10fractions but when tumor measured more than 3 cm (i.e. T2) 70Gy/10fractions was used, and cases that were registered in a certain clinical trial were treated with 48Gy/4fractions. The dose was not constrained by surrounding normal tissues including chest wall. Heterogeneity corrections were made in all cases.

After adjusting the isocenter of the PTV to the planned position in a unit comprising a CT scanner and linear accelerator, irradiation was performed under patient-controlled breath-holding and radiation beam switching.

CT examination

Preradiotherapeutic and follow-up CT were performed using the same 16 multidetector row scanner (Aquilion 16 (Toshiba Medical Systems, Otawara, Japan)) and with the identical protocols.

Parameters for CT scanning were as follows: peak voltage 120 kVp, tube rotation time 0.5 second, slice collimation 1.0 mm, and beam pitch 0.94. Tube currents were determined by an automatic exposure control with the noise factor for determining the applied tube current was set at 11 (standard deviation) and the tube currents actually ranging from 110 to 400 mA.

Contrast-enhanced CT was performed for 116 patients (67.1%) after unenhanced CT. Contrast material (Omnipaque 300, Daiichi Sankyo, Tokyo) in a volume tailored to the body weight of each patient (600 mg iodine/kg body weight) was injected from the anterior cubital vein within a fixed injection time of 50 s (i.e. injection rate was variable.). CT scans were started at 60 and 120 s after beginning of the contrast injection.

These data were reconstructed into 5 mm sections. Thin-section CT (slice thickness, 1 mm) was also produced for regions that included tumor or radiation-induced opacities targeting the affected lung, which was mainly used for the evaluation of chest wall injury.

Preradiotherapeutic CT was performed within 1 month before SRT, while follow-up CT was performed at 3 and 6 months after the completion of the radiotherapy, and every 6 months thereafter.

CT evaluation

Preradiotherapeutic CT was interpreted by either of two chest radiologists (A.N, E.S) in our institution. Maximum tumor size and the shortest distance between the tumor margin and chest wall (tumor-chest wall distance) were measured on 1 mm contrast-enhanced CT with a reconstruction kernel for viewing lung parenchyma as a part of the radiology report. Maximum tumor size was defined as the maximum dimension of a tumor in all of axial CT sections that included the tumor.

Follow-up CT was also examined by either of the same radiologists with special attention to abnormal findings of the chest wall in addition to routine radiological assessment. Rib fracture in this study was defined as a disruption of cortical continuity with malalignment. Thinning of cortex was defined as a focal area of cortex with a thickness less than half of the surrounding normal cortex. Osteosclerosis was defined as an area of increased attenuation comparable to cortex in the medulla of rib.

The time at which each finding first appeared after the completion of SRT was reviewed. Final outcomes of rib

Table 1 Characteristics of the 177 primary lung cancer patients enrolled in this study

	Lung cancer patients (n = 177)
*Average age(range)	77.3 ± 7.0 (55-92)
*Gender (male: female)	132:45
**Range of follow-up period (median)	11-99 (27)
Tumor diameter (average ± standard deviation)	8-55 mm(30.0 ± 9.1)
central tumors: peripheral tumors	22:155
Method of radiotherapy (48Gy/4fr:60Gr/10fr:70Gr/10fr)	75:37:65

*Presented as mean ± standard deviation.

**Presented as median.

fractures during the follow-up period were also assessed on follow-up CT.

Follow-up of patients

Every patient was basically asked to visit our clinic at 3, 6, and every 6 months thereafter after the completion of radiotherapy. At every visit, a thorough examination was performed, consisting of inquiry focusing on pain at the chest wall near the irradiated tumor and respiratory symptoms, physical examination by an attending radiation oncologist, blood test, and CT. Clinical symptoms considered related to chest wall injury after SRT were graded according to the criteria for pain in Common Terminology Criteria for Adverse Events, *version. 3*. Chest radiologists interpreted the results of CT just after the examinations. If the patient complained of pain, analgesics were prescribed as appropriate.

Evaluation of dosimetry

Among the 177 patients, detailed dosimetries were available for review in 26 patients with rib fracture and 22 patients without. Patients without fracture were randomly sampled among those with no evidence of fracture on CT for more than 30 months. We set this period as a cut-off point as most rib fractures after SRT in this series had occurred within 30 months after completion of SRT. At the point on the chest wall that had received the maximum dose, BED was calculated in each case assuming the α/β ratio as 3 (BED_3) (Figure 1). The chest wall volume (cc) that received in $BED_3 \geq 50$ Gy was also calculated.

Data analysis

Data analyses were performed retrospectively using the prospectively interpreted radiology reports.

First, we calculated the crude incidence of rib fracture after SRT on follow-up CT during the follow-up periods of the patients. As crude incidence may underestimate actual incidence of rib fracture, we also performed a Kaplan-Meier method to obtain a more accurate estimate of incidence of rib fracture. We also assessed the relationship between rib fracture and related findings in terms of time frame.

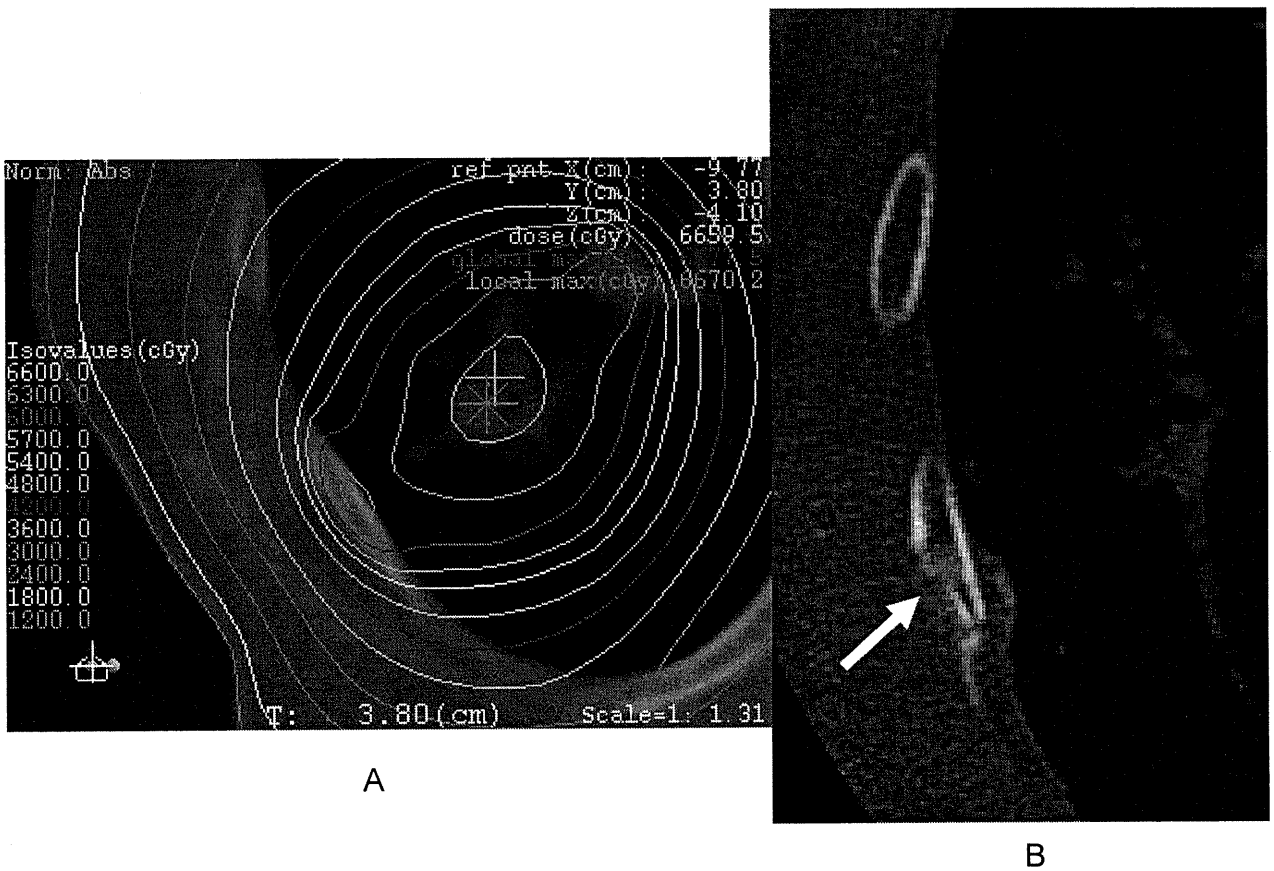

Figure 1 An 86-year old woman with adenocarcinoma. A:Dosimetry overlaying CT shows the maximum prescribed dose of chest wall as 63Gy, with a BED_3 of 233.2Gy. B: Rib fracture was noted at 24 months after completion of SRT. Amorphous osteosclerosis is also seen (arrow).

Second, we determined the threshold tumor-chest wall distance on preradiotherapeutic CT to discriminate patients who with rib fractures from those without. Frequencies of rib fracture when the tumor-chest wall distance was less than or equal to the threshold distance and when the distance was 0 mm were also calculated.

Third, we evaluated the frequency of clinical symptoms.

Fourth, mean BED_3 and $BED_3 \geq 50$ Gy were calculated in fracture and non-fracture groups and were compared between the two groups using unpaired t test. Fisher's exact test or χ^2 test was used to see differences between groups.

Value of $p < 0.05$ were considered statistically significant.

All statistical analyses were performed using IBM SPSS Statistics version 18(New York, USA).

Results

Frequency of rib fractures after SRT

The crude incidence of rib fracture was 23.2% (41/177) at a median follow-up of 27 months (Table 2). The frequency of rib fracture was not statistically different among the three different dose fractionations ($\chi 2$ test, p = 0.391). Kaplan-Meier method estimated the incidence to be 27.4% at 24 months.

Imaging findings of rib fracture and related findings and appearance times

Results of appearance time and frequency of rib fractures are summarized in Table 2. Rib fractures appeared at a mean of 21.2 months (range, 4 -58 months) on follow-up CT. Fractures invariably occurred at the ribs close to the irradiated tumor, and were solitary or multiple (Figure 2). Final outcomes for fractures were non-union in 28 patients, including 14 patients with pseudoarthrosis (defined as covering of cortex over the fractured surface), and bony union in 13. Chest wall edema was seen in 45 of 177 patients (25.4%), appearing at a mean of 12 months after SRT (range, 2 -57 months). Such edema was seen as asymmetrical swelling of the ipsilateral chest wall compared with the contralateral chest wall along with effacement of interlaced intramuscular fat attenuation. Low-attenuation areas in the chest wall were occasionally associated, which became more conspicuous on contrast- enhanced CT (Figure 3). Thinning of the cortex was observed in 36 patients (30.3%) at 4 to 36 months. Osteosclerosis was evident in 26 patients (14.7%) on follow-up CT at a mean of 15 months (range, 4-57 months). This finding appeared as mottled sclerosis of the affected bone (Figure 4). These findings related to rib fracture typically preceded the identification of rib fracture.

Symptoms of rib fracture

Clinical symptoms in patients with rib fracture and without rib fracture are summarized in Table 3. Chest wall pain was seen in 18 of 177 patients (10.2%), of whom 14 patients developed rib fracture. No patients complained of Grade 3 or more symptoms. Four patients without rib fractures complained of Grade 1 chest wall pain with all 4 cases showing radiological evidence of chest wall edema. In the study population as a whole, the frequency of chest wall pain was 21.5% (38/177). The frequency of chest wall pain was not significantly different between the patients with union (6/13, 46%) and non-union (7/28, 25%) rib fracture (Fisher's exact test, p = 0.160).

Threshold tumor-chest wall distance in the occurrence of rib fracture

Mean tumor-chest wall distance was 12.3 mm (range, 0 - 53 mm). No patients with rib fracture showed a tumor-chest wall distance > 16 mm, while frequency of rib fracture was 31.3% (41/131) for a distance ≤ 16 mm, and 37.1% at 24 months by Kaplan-Meier method. When the distance was 0 mm, frequency of rib fracture was 36.7% (22/60) and 51.8% at 24 months by Kaplan-Meier method (Table 4).

Maximum BED3 of the chest wall in patients with and without rib fracture, and threshold dose for rib fracture occurrence Mean BED3 of the chest wall was 240.7 ± 38.7 in 26 patients with rib fracture and 146.8 ± 74.5 in 22 patients without rib fracture, representing a significant difference between groups (p < 0.001). The lowest BED3 that resulted in rib fracture was 152.4 Gy. Mean

Table 2 Appearance time and frequencies of the rib fractures and related findings

	Appearance time ranges (months)*	Crude frequency of each finding	Frequency at 24 months by Kaplan-Meier method
Rib fracture	21.2 (4-58)	41/177(23.2%)	27.4%
Thinning of the cortex	15.6 (4-36)	36/177 (20.3%)	
Osteosclerosis	14.7 (4-57)	26/177(14.7%)	
Chest wall edema	12.0 (2-57)	45/177 (25.4%)	

*Presented as mean (range).

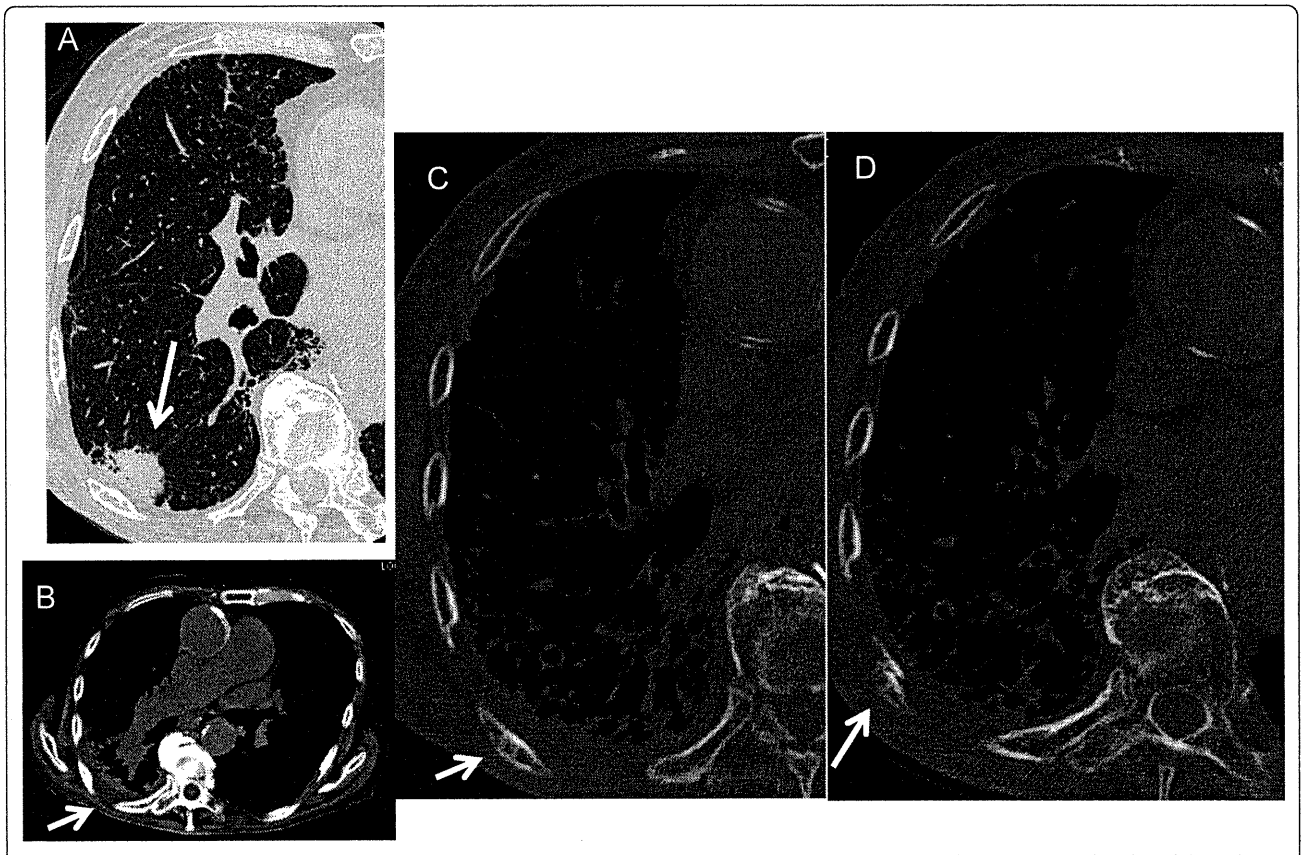

Figure 2 An 85-year-old man with a rib fracture after SRT. A, A preradiotherapeutic thin-section CT showing a spiculated nodule with air-containing spaces (arrow). B, Seven months later after SRT, CT shows edema of the right chest wall adjacent to the tumor, as evidenced by asymmetrical swelling and effacement of the fat planes (arrow). C, On follow-up CT at 13 months after SRT, thin-section CT with a bone window setting demonstrates thinning of cortex with mild sclerotic foci of the medulla in a rib. D, At 20 months after SRT, rib fracture with malalignment of the cortex is apparent (arrow).

chest wall volume (cc) with BED3 > 50Gy was 110.3 ± 45.0cc in the fracture group and 50.1 ± 59.8 in the non-fracture group, again representing a significant difference ($p < 0.001$). The minimum volume that resulted in rib fracture was 25cc.

Discussion

Our results demonstrated that the development of rib fracture after SRT is not uncommon with a frequency of 23.2% for the whole study population. Not unexpectedly, frequency increased with closer proximity of the tumors to the chest wall, from 31.3% ≤16 mm to 36.7% at 0 mm. The reported frequencies of rib fracture after SRT vary widely among investigators, ranging from 3% to 21.2% [5-7,13-16]. Our result is closest to that reported by Petterson, et al., who reported the highest frequency (21.2%) among the previous reports [14]. We speculate that these discrepancies are mainly caused by differences in the methods for estimating frequency. Petterson, et al. and the present study obtained frequencies based on follow-up CT, whereas other studies based frequencies on findings for patients who complained symptoms. That is, differences may be largely due to whether asymptomatic patients with rib fracture were likely to be included in frequency calculations. Our clinical experience supports this speculation. Differences in follow-up periods, methods of SRT or the proportion of tumors close to the chest wall may also have contributed to the discrepancies between studies. The frequency of rib fracture reported by Petterson, et al. is still lower than our result despite the fact that they used a higher prescribed SRT dose than we did. This may be because thin-section CT in the present study may have allowed sensitive detection of rib fracture.

In Kaplan-Meier method, the frequency of rib fracture was calculated to be even higher (27.4% at 24 months). This incidence is considered to be a more accurate estimate of frequency of rib fracture as there were censored cases during the follow-up periods.

The frequency of rib fracture is also more common in SRT for lung cancer than in breast conserving surgery combined with radiotherapy, which has a reported frequency of 0.3-2.2% [17,18], probably due to much higher

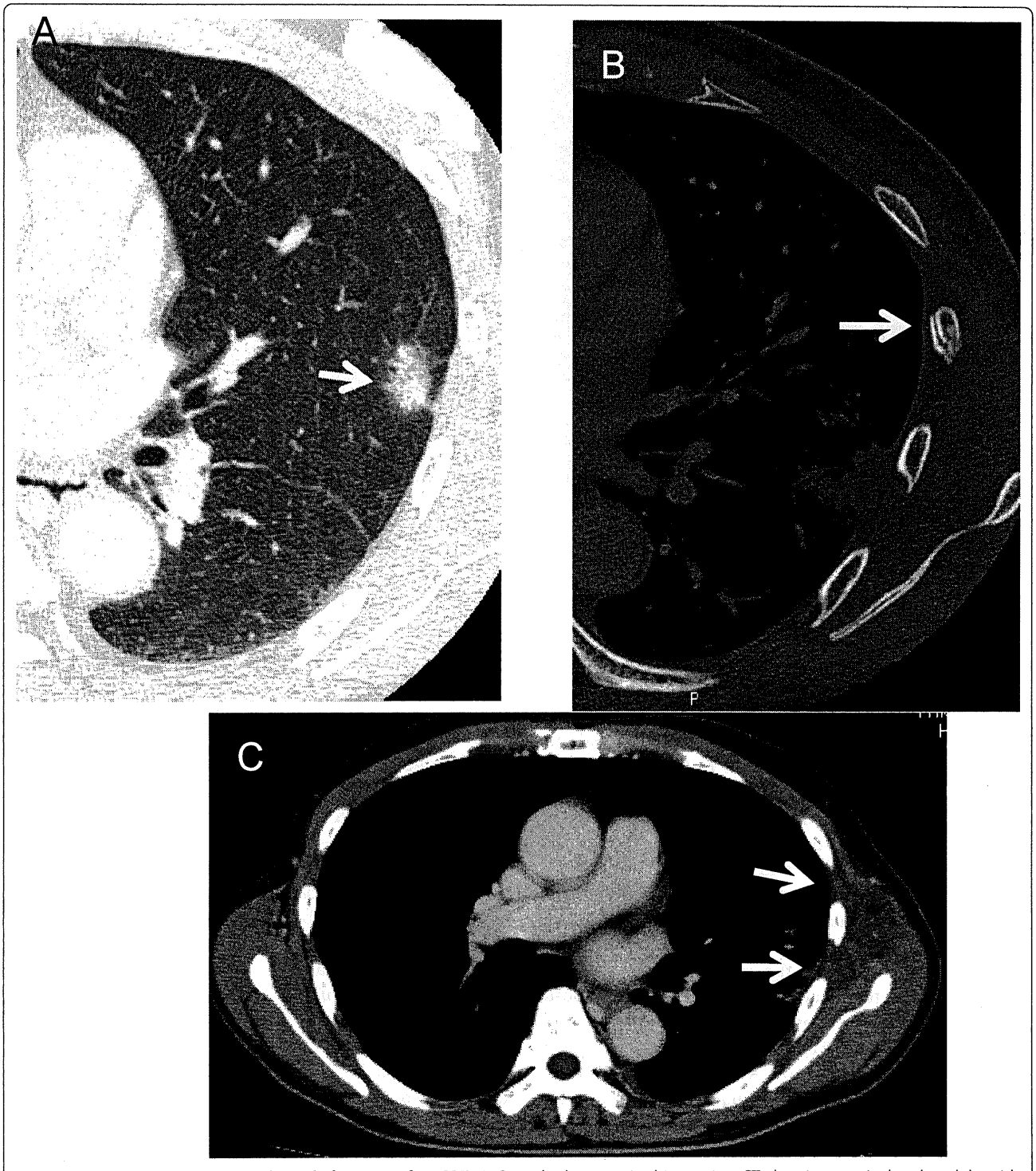

Figure 3 A 65-year-old man with a rib fracture after SRT. A, Preradiotherapeutic thin-section CT showing a spiculated nodule with surrounding ground-glass opacity close to the chest wall (arrow). B, Twelve months later after SRT, a rib fracture is apparent (arrow). C, At 6 months after SRT, enhanced CT shows swelling of the left chest wall with an area of low attenuation (arrows).

dose delivered to the rib in SRT when tumors are close to the chest wall.

Rib fractures occurred at a mean of 21.2 months (range, 4-58 months) after SRT, mostly within 30 months after completion of SRT, and were frequently preceded by chest wall edema, thinning of the cortex of the rib or sclerosis of the medulla of the rib. We may summarize the typical course of chest wall injury after

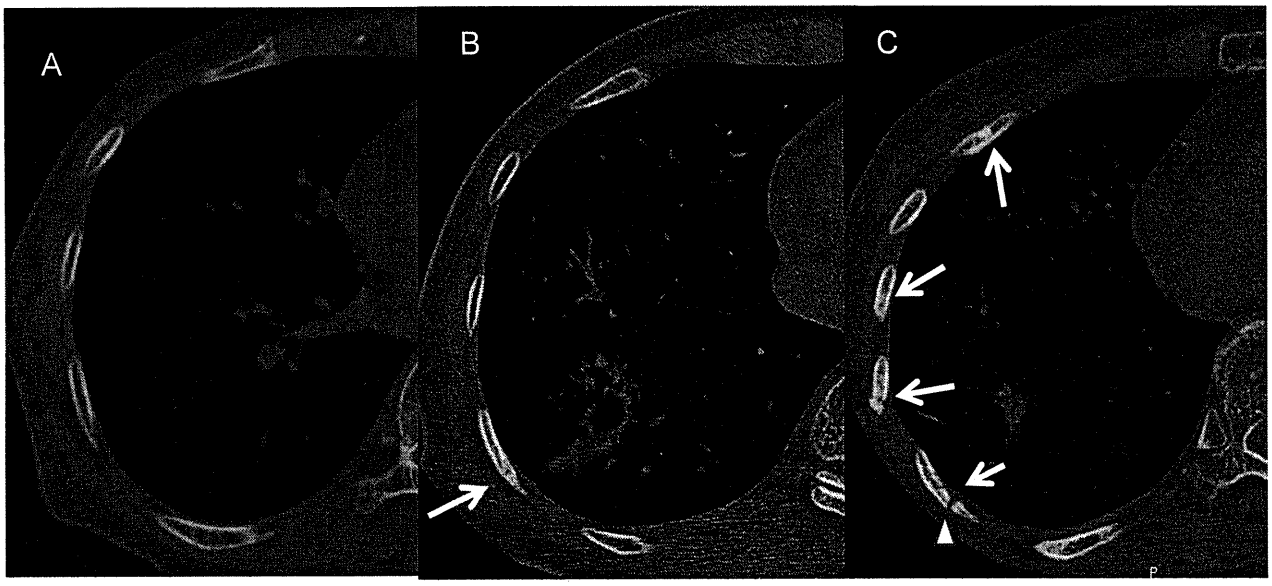

Figure 4 A 85-year-old woman with adenocarcinoma. A, Preradiotherapeutic thin-section CT at the bone window shows no marked abnormality of the ribs. B, At 18 months after SRT, bone sclerosis of the rib adjacent to the lung tumor appeared (arrow). C, At 30 months after completion of SRT, multiple rib fractures with areas of sclerosis are seen. Pseudoarthrosis is present in one of the fractured bones (arrow head).

SRT as depicted on thin-section CT as follows: at several months after SRT chest wall edema first appears. The cortex then becomes thinner and the medulla sometimes becomes sclerotic in a mottled fashion, and the affected rib eventually undergoes fracture. These CT findings presumably correspond to soft tissue edema and changes in bone vascularity due to increased permeability or occlusion of the capillaries caused by irradiation of the soft tissue, and a decrease in number of osteoblasts resulting in decreased collagen production, in turn causing osteopenia and subsequent bone injury [19]. Osteosclerosis after radiotherapy is considered to represent reactive bone formation caused by remaining osteoblast cells [20].

Under such conditions, the rib becomes extremely vulnerable and often fractures. Although these bone changes may actually represent insufficiency fracture [19], radiation osteitis [21], callous formation secondary to microtrabecular fracture or osteonecrosis [22], we did not use these terms as we had no pathological confirmation of such findings. We therefore employed the common terms for imaging findings.

Table 3 Frequency and degree of chest wall pain

Degree of pain*	Fracture group (n = 41)	Non-fracture group (n = 136)
Grade 0	27 (65.9)	132(97)
Grade 1	7 (17.1)	4(3)
Grade 2	7 (17.1)	0(0)
Grade 3 and 4	0 (0)	0(0)

*The degree of chest wall pain was evaluated according to Common Terminology Criteria for Adverse Events, *Ver. 3*.

**The numbers in the parentheses are percentages

We think that these preceding findings may be usable as predictors of rib fracture. Prediction of rib fracture may be informative to the referring physicians as well as to patients as we might initiate treatment for chest wall pain related to the forthcoming rib fracture in advance or possibly take some preventive measures against rib fractures. Although the frequency of clinical symptoms was not high in patient with rib fracture and the clinical symptoms were generally not severe, most symptomatic patients had rib fracture. Therefore, prediction of rib fracture will clinically be important.

In addition, bone sclerosis or focal loss of cortex may be mistaken for metastasis. Familiarity with these findings will therefore minimize the potential for confusion.

The outcomes of rib fracture were non-union in 28 patients, including 14 patients with pseudoarthrosis and bony union in 13. Needless to say, the proportion of union and non-union largely depends on the duration of follow-up and the prescribed dose to tumors. However, we can at least say that a substantial proportion of rib fractures after SRT for lung cancer can remain a state of non-union for a long time after SRT and that pseudoarthrosis is not uncommon. However, the outcomes of rib fracture seem unrelated to the frequency of clinical symptoms.

A tumor-chest wall distance of 16 mm appears to represent a threshold value, beyond which rib fracture did not occur, in our series. This threshold offers a concise and convenient reference value. Undoubtedly, the

Table 4 Frequency of rib fracture in relation to tumor-chest wall distance

Tumor-chest wall distance(mm)	Crude frequency	Frequency at 24 months by Kaplan-Meier method
≤25	41/148(27.8%)	33.2%
≤16	30/131(31.3%)	37.1%
0	22/60(36.7%)	51.8%

*The numbers in the parentheses in frequency are percentages.

risk of rib fractures depends much more on the dose delivered to the rib and therefore a dosimetry-based evaluation can provide a more accurate estimate of the risk of rib fractures. However, dosimetry can only be produced after SRT is chosen as the treatment. Our approach can provide a patient or referring physician with information about the risk of rib fracture based only on preradiotherapeutic CT before decision is made to undergo SRT. Our result may not be simply applicable to patients in other institutions as prescribed doses differ among institutions, but will be valid when prescribed doses are less than or equal to our own.

Mean BED_3 of the chest wall (240.7 ± 38.7 Gy) and mean chest wall volume (cc) with $BED_3 \geq 50Gy$ (110.3 ± 45.0cc) in 26 patients with rib fracture were much higher than those (146.8 ± 74.5Gy and 50.1 ± 59.8cc) in 22 patients without rib fracture, with statistical significances, respectively. These values may also be usable to predict the risk of rib fracture. The lowest BED_3 that resulted in rib fracture was 152.4Gy. The threshold BED_3 for producing rib fracture seemed to be around 150Gy, but further investigation is necessary to make a definitive conclusion.

This study has some limitations that must be considered. First, we regarded the appearance time of rib fracture and other related findings as that when these findings were first seen on follow-up CT. However, these events would actually have occurred within the interval of time since the previous CT. The present study would thus have overestimated time that elapsed until these events.

Second, for BED_3 of chest wall, only a small number of cases from the study population were sampled. This was because of the limited capability of our treatment planning computer for data handling, which requires a substantial amount of time to reproduce a dosimetry. Calculating dosimetries of all cases is obviously the best way to obtain a threshold BED, but we believe that our random sampling method provided a clear and concise reference value, which would offer a benchmark when considering risk of rib fracture in clinical practice. Third, the method of SRT for lung cancer has yet to be standardized. So, our results cannot be simply applied to other institutions.

Conclusion

Rib fracture is seen with high frequency after SRT for lung cancer when the tumor is close to the chest wall. Chest wall edema and thinning and osteosclerosis of the cortex represent related findings that often precede rib fracture and might be predictive of a forthcoming rib fracture. However, related chest wall pain is less frequent and is generally mild if present.

Author details
[1]Department of Radiology, University of Yamanashi, Chuo City, Japan. [2]Department of Radiology, Kofu Municipal Hospital, Kofu City, Japan. [3]Department of Radiology, Yamanashi Prefectural Central Hospital, Kofu City, Japan.

Authors' contributions
All authors approved read and approved the final version of this paper. AN is the first author of this paper involved in interpretation of CT, clinical data collection, statistical analysis and drafting this paper. HO carried out clinical data collection, supervision of this study, editing and approving the paper. SA carried out clinical data collection, dosimetry calculation and revision of clinical data. TK, ES and LT carried out collection of CT data and clinical data. KK, TK, KM, MA, RS and YM carried out clinical evaluations of patient at follow-up visits. TA carried out supervision of this study and final approval of this paper.

Competing interests
The authors declare that they have no competing interests.

Received: 10 July 2011 Accepted: 13 October 2011
Published: 13 October 2011

References

1. Uematsu M, Shioda A, Suda A, Fukui T, Ozeki Y, Hama Y, Wong JR, Kusano S: **Computed tomography-guided frameless stereotactic radiotherapy for stage I non-small cell lung cancer: a 5-year experience.** *Int J Radiat Oncol Biol Phys* 2001, **51**:666-670.
2. Onishi H, Araki T, Shirato H, Nagata Y, Hiraoka M, Gomi K, Yamashita T, Niibe Y, Karasawa K, Hayakawa K, Takai Y, Kimura T, Hirokawa Y, Takeda A, Ouchi A, Hareyama M, Kokubo M, Hara R, Itami J, Yamada K: **Stereotactic hypofractionated high-dose irradiation for stage I nonsmall cell lung carcinoma: clinical outcomes in 245 subjects in a Japanese multiinstitutional study.** *Cancer* 2004, **10**:1623-1631.
3. Nagata Y, Takayama K, Matsuo Y, Norihisa Y, Mizowaki T, Sakamoto T, Sakamoto M, Mitsumori M, Shibuya K, Araki N, Yano S, Hiraoka M: **Clinical outcomes of a phase I/II study of 48 Gy of stereotactic body radiotherapy in 4 fractions for primary lung cancer using a stereotactic body frame.** *Int J Radiat Oncol Biol Phys* 2005, **63**:1427-1431.
4. Onishi H, Shirato H, Nagata Y, Hiraoka M, Fujino M, Gomi K, Niibe Y, Karasawa K, Hayakawa K, Takai Y, Kimura T, Takeda A, Ouchi A, Hareyama M, Kokubo M, Hara R, Itami J, Yamada K, Araki T: **Hypofractionated stereotactic radiotherapy (HypoFXSRT) for stage I non-small cell lung cancer: updated results of 257 patients in a Japanese multi-institutional study.** *J Thorac Oncol* 2007, **2(7 Suppl 3)**:94-100.
5. Nyman J, Johansson KA, Hultén U: **Stereotactic hypofractionated radiotherapy for stage I non-small cell lung cancer–mature results for medically inoperable patients.** *Lung Cancer* 2006, **51**:97-103.
6. Zimmermann FB, Geinitz H, Schill S, Thamm R, Nieder C, Schratzenstaller U, Molls M: **Stereotactic hypofractionated radiotherapy in stage I (T1-2 N0 M0) non-small-cell lung cancer (NSCLC).** *Acta Oncol* 2006, **45**:796-801.

7. Fritz P, Kraus HJ, Blaschke T, Mühlnickel W, Strauch K, Engel-Riedel W, Chemaissani A, Stoelben E: **Stereotactic, high single-dose irradiation of stage I non-small cell lung cancer (NSCLC) using four-dimensional CT scans for treatment planning.** *Lung Cancer* 2008, **60**:193-199.
8. Haasbeek CJ, Lagerwaard FJ, de Jaeger K, Slotman BJ, Senan S: **Outcomes of stereotactic radiotherapy for a new clinical stage I lung cancer arising postpneumonectomy.** *Cancer* 2009, **115**:587-594.
9. Inoue T, Shimizu S, Onimaru R, Takeda A, Onishi H, Nagata Y, Kimura T, Karasawa K, Arimoto T, Hareyama M, Kikuchi E, Shirato H: **Clinical outcomes of stereotactic body radiotherapy for small lung lesions clinically diagnosed as primary lung cancer on radiologic examination.** *Int J Radiat Oncol Biol Phys* 2009, **75**:683-687.
10. Onishi H, Shirato H, Nagata Y, Hiraoka M, Fujino M, Gomi K, Karasawa K, Hayakawa K, Niibe Y, Takai Y, Kimura T, Takeda A, Ouchi A, Hareyama M, Kokubo M, Kozuka T, Arimoto T, Hara R, Itami J, Araki T: **Stereotactic Body Radiotherapy (SBRT) for Operable Stage I Non-Small-Cell Lung Cancer: Can SBRT Be Comparable to Surgery?** *Int J Radiat Oncol Biol Phys* 2010.
11. Barriger RB, Forquer JA, Brabham JG, Andolino DL, Shapiro RH, Henderson MA, Johnstone PA, Fakiris AJ: **A Dose-Volume Analysis of Radiation Pneumonitis in Non-Small Cell Lung Cancer Patients Treated with Stereotactic Body Radiation Therapy.** *Int J Radiat Oncol Biol Phys* 2010.
12. Takeda A, Ohashi T, Kunieda E, Enomoto T, Sanuki N, Takeda T, Shigematsu N: **Early graphical appearance of radiation pneumonitis correlates with the severity of radiation pneumonitis after stereotactic body radiotherapy (SBRT) in patients with lung tumors.** *Int J Radiat Oncol Biol Phys* 2010, **77**:685-690.
13. Dunlap NE, Cai J, Biedermann GB, Yang W, Benedict SH, Sheng K, Schefter TE, Kavanagh BD, Larner JM: **Chest wall volume receiving > 30 Gy predicts risk of severe pain and/or rib fracture after lung stereotactic body radiotherapy.** *Int J Radiat Oncol Biol Phys* 2010, **76**:796-801.
14. Pettersson N, Nyman J, Johansson KA: **Radiation-induced rib fractures after hypofractionated stereotactic body radiation therapy of non-small cell lung cancer: a dose- and volume-response analysis.** *Radiother Oncol* 2009, **91**:360-368.
15. Voroney JP, Hope A, Dahele MR, Purdie TG, Franks KN, Pearson S, Cho JB, Sun A, Payne DG, Bissonnette JP, Bezjak A, Brade AM: **Chest wall pain and rib fracture after stereotactic radiotherapy for peripheral non-small cell lung cancer.** *J Thorac Oncol* 2009, **4**:1035-1037.
16. Milano TMichael, Constine SLouis, Okunieff Paul: **Normal tissue toxicity after small field hypofractionated stereotactic body radiation.** *Radiation Oncology* 2008, **3**:36.
17. Pierce SM, Recht A, Lingos TI, Abner A, Vicini F, Silver B, Herzog A, Harris JR: **Long-term radiation complications following conservative surgery (CS) and radiation therapy (RT) in patients with early stage breast cancer.** *Int J Radiat Oncol Biol Phys* 1992, **23**:915-923.
18. Meric F, Buchholz TA, Mirza NQ, Vlastos G, Ames FC, Ross MI, Pollock RE, Singletary SE, Feig BW, Kuerer HM, Newman LA, Perkins GH, Strom EA, McNeese MD, Hortobagyi GN, Hunt KK: **Long-term complications associated with breast-conservation surgery and radiotherapy.** *Ann Surg Oncol* 2002, **9**:543-549.
19. Bluemke DA, Fishman EK, Scott WW Jr: **Skeletal complications of radiation therapy.** *Radiographics* 1994, **14**:111-121.
20. Kwon JW, Huh SJ, Yoon YC, Choi SH, Jung JY, Oh D, Choe BK: **Pelvic bone complications after radiation therapy of uterine cervical cancer: evaluation with MRI.** *AJR Am J Roentgenol* 2008, **191**:987-994.
21. Bragg DG, Shidnia H, Chu FC, Higinbotham NL: **The clinical and radiographic aspects of radiation osteitis.** *Radiology* 1970, **97**:103-111.
22. Hoff AO, Toth B, Hu M, Hortobagyi GN, Gagel RF: **Epidemiology and risk factors for osteonecrosis of the jaw in cancer patients.** *Ann N Y Acad Sci* 2010.

doi:10.1186/1748-717X-6-137
Cite this article as: Nambu *et al.*: Rib fracture after stereotactic radiotherapy on follow-up thin-section computed tomography in 177 primary lung cancer patients. *Radiation Oncology* 2011 **6**:137.

Int. J. Radiation Oncology Biol. Phys., Vol. 81, No. 5, pp. 1352–1358, 2011

0360-3016/$ - see front matter

ELSEVIER

doi:10.1016/j.ijrobp.2009.07.1751

CLINICAL INVESTIGATION **Lung**

STEREOTACTIC BODY RADIOTHERAPY (SBRT) FOR OPERABLE STAGE I NON–SMALL-CELL LUNG CANCER: CAN SBRT BE COMPARABLE TO SURGERY?

Hiroshi Onishi, M.D.,* Hiroki Shirato, M.D.,† Yasushi Nagata, M.D.,‡ Masahiro Hiraoka, M.D.,§ Masaharu Fujino, M.D.,†* Kotaro Gomi, M.D.,‖ Katsuyuki Karasawa, M.D.,¶ Kazushige Hayakawa, M.D.,# Yuzuru Niibe, M.D.,# Yoshihiro Takai, M.D.,** Tomoki Kimura, M.D.,†† Atsuya Takeda, M.D.,‡‡ Atsushi Ouchi, M.D.,§§ Masato Hareyama, M.D.,‖‖ Masaki Kokubo, M.D.,¶¶ Takuyo Kozuka, M.D.,## Takuro Arimoto, M.D.,*** Ryusuke Hara, M.D.,††† Jun Itami, M.D.,‡‡‡ and Tsutomu Araki, M.D.*

*School of Medicine, Yamanashi University, Yamanashi, Japan; †School of Medicine, Hokkaido University, Sapporo, Japan; ‡School of Medicine, Hiroshima University, Hiroshima, Japan; §School of Medicine, Kyoto University, Kyoto, Japan; ‖Cancer Institute Suwa Red-Cross Hospital, Suwa, Japan; ¶Tokyo Metropolitan Komagome Hospital, Tokyo, Japan; #Kitasato University, Kanagawa, Japan; **School of Medicine, Hirosaki University, Hirosaki, Japan; ††School of Medicine, Kagawa University, Hiroshima, Japan; ‡‡Ofuna Chuo Hospital, Kanagawa, Japan; §§Keijinkai Hospital, Sapporo, Japan; ‖‖Sapporo Medical University, Sapporo, Japan; ¶¶Institute of Biomedical Research and Innovation, Kobe, Japan; ##School of Cancer Institute Ariake Hospital, Tokyo, Japan; ***Kitami Red Cross Hospital, Kitami, Japan; †††National Institute of Radiological Science, Chiba, Japan; and ‡‡‡National Cancer Center, Tokyo, Japan

Purpose: To review treatment outcomes for stereotactic body radiotherapy (SBRT) in medically operable patients with Stage I non–small-cell lung cancer (NSCLC), using a Japanese multi-institutional database.

Patients and Methods: Between 1995 and 2004, a total of 87 patients with Stage I NSCLC (median age, 74 years; T1N0M0, *n* = 65; T2N0M0, *n* = 22) who were medically operable but refused surgery were treated using SBRT alone in 14 institutions. Stereotactic three-dimensional treatment was performed using noncoplanar dynamic arcs or multiple static ports. Total dose was 45–72.5 Gy at the isocenter, administered in 3–10 fractions. Median calculated biological effective dose was 116 Gy (range, 100–141 Gy). Data were collected and analyzed retrospectively.

Results: During follow-up (median, 55 months), cumulative local control rates for T1 and T2 tumors at 5 years after SBRT were 92% and 73%, respectively. Pulmonary complications above Grade 2 arose in 1 patient (1.1%). Five-year overall survival rates for Stage IA and IB subgroups were 72% and 62%, respectively. One patient who developed local recurrences safely underwent salvage surgery.

Conclusion: Stereotactic body radiotherapy is safe and promising as a radical treatment for operable Stage I NSCLC. The survival rate for SBRT is potentially comparable to that for surgery. © **2011 Elsevier Inc.**

Stereotactic body radiotherapy, Lung cancer, Non–small-cell, Operable, Stage I.

INTRODUCTION

With the popularization of computed tomography (CT) screening, lung cancers are increasingly detected at an early stage. For patients with Stage I (T1 or 2, N0, M0) non–small-cell lung cancer (NSCLC), resection of the set of full lobar and systemic lymph nodes represents standard treatment. Five-year overall survival rates for clinical Stage IA and IB treated surgically are approximately 60–75% and 40–60%, respectively (1–3). However, a proportion of patients who meet the criteria for surgery refuse such intervention for various reasons. Radiotherapy offers a therapeutic alternative in such cases, but the effects of conventional radiotherapy in patients with Stage I NSCLC are unsatisfactory, with local control rates of approximately 50% during a short 5-year survival period in 15–30% of patients (4–7). Survival rates for conventional radiotherapy for a statistically sufficient number of cases of operable Stage I NSCLC have not been reported, because most

Reprint requests: Hiroshi Onishi, M.D., Department of Radiology, School of Medicine, University of Yamanashi, 1110 Shimokato, Chuo City, Yamanashi 409-3898, Japan. Tel: (+81) 55-273-1111, ext 2382; Fax: (+81) 55-273-6744; E-mail: honishi@yamanashi.ac.jp

Presented at the 43rd Annual Meeting of the American Society of Clinical Oncology, June 1–7, 2007, Chicago, IL; and the 49th Annual Meeting of the American Society of Therapeutic Radiology and Oncology, October 28–November 1, 2007, Los Angeles, CA.

Supported in part by a Grant-in-Aid from the Ministry of Health, Welfare and Labor of Japan.

Conflict of interest: none.

Acknowledgments—The authors thank the patients and staff who assisted in this study.

Received May 7, 2009, and in revised form July 21, 2009. Accepted for publication July 22, 2009.

patients receiving radiotherapy are inoperable. The poor local control rates with conventional radiotherapy have been attributed to doses of conventional radiotherapy that are too low to control the tumor. Mehta *et al.* (8) provided a detailed theoretical analysis of NSCLC responses to radiotherapy and a rationale for dose escalation. They concluded that higher biologically effective doses (BED) irradiated during a short period must be administered to achieve successful local control of lung cancer. To provide a higher dose to the tumor without increasing adverse effects, three-dimensional conformal radiotherapy techniques have been used, and better local control and survival have recently been reported (9–11). Over the last decade, hypofractionated high-dose stereotactic body radiotherapy (SBRT) has been actively performed for early-stage lung cancer, particularly in Japan (12–17). We have previously reported preliminary results for a Japanese multi-institutional review of 257 patients with Stage I NSCLC treated with SBRT (18). The results showed that local control and survival rates were better with BED ≥100 Gy than with <100 Gy, and survival rates were much better for medically operable patients than for medically inoperable patients. These results were encouraging, but the duration of follow-up for the study was somewhat short (median, 38 months), and we have not presented a detailed analysis of medically operable patients as a distinct subgroup. Although the standard therapy for operable Stage I NSCLC remains surgery, the effect of SBRT on medically operable patients is an issue of great concern. We provide herein detailed and matured results of SBRT (BED ≥100 Gy) for medically operable patients with Stage I NSCLC, using a retrospectively collected Japanese multi-institutional database.

PATIENTS AND METHODS

Eligibility criteria

All patients who satisfied the following eligibility criteria were retrospectively collected from 14 major Japanese institutions in which SBRT for lung cancer was actively performed: (*1*) identification of T1N0M0 or T2N0M0 primary lung cancer on chest and abdominal CT, bronchoscopy, bone scintigraphy, or brain magnetic resonance imaging; (*2*) histopathologic confirmation of NSCLC; (*3*) medically operable cancer but selection of SBRT after refusal to undergo surgery. Medical operability was discussed within the multidisciplinary tumor board of each institution according to respiratory function, age, and complicating diseases. Basic cutoff values for medical operability were World Health Organization performance status ≤2, pressure of arterial oxygen ≥65 mm Hg, predicted postoperative forced expiratory volume in 1 s ≥800 mL, no heart failure requiring pharmacotherapy, no diabetes requiring insulin, no severe arrhythmia, and no history of cardiac infarction. Positron emission tomography was not essential in the staging procedures.

Patients were informed of the concept, methodology, and rationale of this treatment, which was performed in accordance with the 1983 revision of the Declaration of Helsinki.

Table 1. Patient characteristics

Number (14 institutions)	87
Male	63
Female	24
Age (y), median (range)	74 (43–87)
ECOG performance status	
0	51
1	30
2	6
Histology	
Adenocarcinoma	54
Squamous cell carcinoma	25
Other	8
Stage	
IA	64
IB	23
Tumor diameter (mm), median (range)	25 (7–50)
IA	21
IB	39
Chronic lung disease	
Positive	38
Negative	49

Abbreviation: ECOG = Eastern Cooperative Oncology Group. Values are number unless otherwise noted.

Patient characteristics

A summary of patient pretreatment characteristics is given in Table 1. From April 1995 to March 2004, a total of 87 medically operable patients with primary NSCLC were treated using hypofractionated high-dose SBRT in 14 major Japanese institutions. Each of these 87 cases was judged medically operable, and surgery was initially recommended, but the patients declined surgery and selected SBRT as a radical treatment. Pathology of all tumors was confirmed as NSCLC by transbronchial or CT-guided percutaneous biopsy. The 14 participating institutions were these: Hokkaido University; Kyoto University; Cancer Institute Hospital; Tokyo Metropolitan Komagome Hospital; Kitasato University; Tohoku University; Hiroshima University; Tokyo Metropolitan Hiroo Hospital; Sapporo Medical University; Institute of Biomedical Research and Innovation; International Medical Center of Japan; Tenri Hospital; Kitami Red Cross Hospital; and Yamanashi University.

Treatment methods

Although the techniques to accomplish stereotactic methods differed among these institutions, all "stereotactic radiotherapy techniques" fulfilled the following five requirements: (*1*) reproducibility of the isocenter (setup error ≤5 mm), as confirmed by image guidance for every fraction; (*2*) respiratory motion (internal margin) suppressed using as much as possible, to <5 mm; (*3*) slice thickness on CT ≤3 mm for three-dimensional treatment planning; (*4*) irradiation with multiple noncoplanar static ports or dynamic arcs; and (*5*) single high dose ≥5 Gy.

Gross target volume (GTV) was delineated on CT images displayed with a lung window level. Clinical target volume (CTV) marginally exceeded GTV by 0–5 mm as judged by the individual radiation oncologist. Internal margin was

calculated and set around the CTV by 2–5 mm according to the individual measurements for respiratory motion of each institution. Internal margin caused by respiratory motion was reduced by gating, tracking, breath-hold technique, or abdominal compression. Planning target volume (PTV) comprised the CTV, a proper internal margin measured in each patient, and a 5-mm safety margin. The total margin between PTV and GTV was thus 7–15 mm. The irradiated port marginally exceeded PTV by 3–5 mm to secure the surface dose of PTV. Dose calculation was performed using the Clarkson algorithm and heterogeneity correction. A total dose of 45–72.5 Gy (mean, 58.7 Gy) at the isocenter in 3–10 fractions with single doses of 6.25–15 Gy was administered with 6-MV X-rays within 20% heterogeneity in the PTV dose. Minimum dose in the PTV corresponded to 85–95% of the prescribed dose in most cases. Typical dose/fractionation schedules were 75 Gy in 10 fractions for 42 patients and 48 Gy in 4 fractions for 38 patients. In principal, patients were treated on consecutive days, but some patients were treated every other day. No chemotherapies were administered before or during radiotherapy.

To compare the effects of various treatment protocols with different fraction sizes and total doses, BED was utilized in a linear-quadratic model (19). Biologically effective dose was here defined as $nd(1 + d/\alpha/\beta)$, with units of Gy, where n is fractionation number, d is daily dose, and α/β is assumed to be 10 for tumors. Biologically effective dose was not corrected with values for tumor doubling time or treatment term. Biologically effective dose was calculated at the isocenter in this study. Median calculated BED was 116 Gy (range, 100–141 Gy).

No restriction was placed on whether the tumor was located peripherally or centrally in the lung, but dose for the spinal cord was limited. Biologically effective dose limitation for spinal cord was 80 Gy (α/β was assumed to be 2 Gy for chronic spinal cord toxicity). Doses for other organs were not restricted.

Evaluation

The objectives of this study were to retrospectively evaluate toxicity, local control rate, and survival rate. Follow-up examinations were performed 4 weeks after treatment first, then patients were seen every 1–3 months. Tumor response was evaluated using the Response Evaluation Criteria in Solid Tumors by CT (20). Chest CT (slice thickness, 2–5 mm) was usually obtained every 2 to 3 months for the first year and repeated every 4–6 months thereafter. Complete response indicated that the tumor had completely disappeared or was judged to have been replaced by fibrotic tissue. Partial response was defined as a ≥30% reduction in maximum cross-sectional diameter. Distinguishing between residual tumor tissue and radiation fibrosis was difficult. Any suspicious residual confusing density after radiotherapy was considered evidence of partial response, so actual complete response rate may have been higher than presented herein. Distinguishing between local recurrence and inflammatory change was also difficult. Here, local recurrence was considered to have occurred only when enlargement of the local tumor continued for >6 months on follow-up CT, obviously positive findings were identified on positron emission tomography, or histologic confirmation was acquired. Findings on CT were interpreted by two radiation oncologists in each case. Absence of local recurrence was defined as locally controlled disease. Lung, esophagus, bone marrow, and skin were evaluated using version 2 of the National Cancer Institute–Common Toxicity Criteria.

Statistical analysis

Cumulative rates of progression-free status at local, regional lymph node, and distant sites and survival were calculated and drawn using Kaplan-Meier algorithms, with day of treatment as the starting point. Subgroups were compared using log–rank statistics. Values of $p < 0.05$ were considered statistically significant. Statistical calculations were conducted using StatView version 5.0 software (SAS Institute, Cary, NC).

RESULTS

All patients completed treatment without obvious complaints. Median durations of observation for all patients and survivors as of final follow-up were 55 and 63 months, respectively.

Local tumor response

Complete response was achieved in 28 patients (32.2%), and partial response was seen in 43 patients (49.4%).

Toxicity

Radiation-induced pulmonary complications of National Cancer Institute–Common Toxicity Criteria (version 2.0) Grade 0, 1, 2, and 3 were noted in 21 (24.1%), 61 (70.1%), 4 (4.6%), and 1 patient (1.1%), respectively. Rib fracture and Grade 3 dermatitis were observed in 4 (4.6%) and 3 patients (3.4%), respectively. All tumors bordered the chest wall. Grade 3 radiation-induced esophagitis was produced in 1 patient, in whom the tumor slightly bordered the esophagus. Maximum esophageal dose in this case was 30 Gy in 5 fractions. No vascular, cardiac, or bone marrow complications had been encountered as of last follow-up. In total, Grade 3 toxicities were identified in 8 patients (9.2%).

No definite second malignancies were found during follow-up, but 1 patient died of acute myelogenous leukemia 3.7 years after completing SBRT.

Recurrence

Local recurrence, lymph node metastases, and distant metastases occurred in 8 (9.2%), 13 (14.9%), and 19 cases (21.8%), respectively.

Cumulative local progression–free rate curves according to stage are shown in Fig. 1. Cumulative local progression–free rate after 5 years was 86.7% (95% confidence interval [CI], 78.3–94.9%) for total cases. Cumulative local progression–free rate at 5 years was 92.0% (95% CI, 83.8–99.6%)

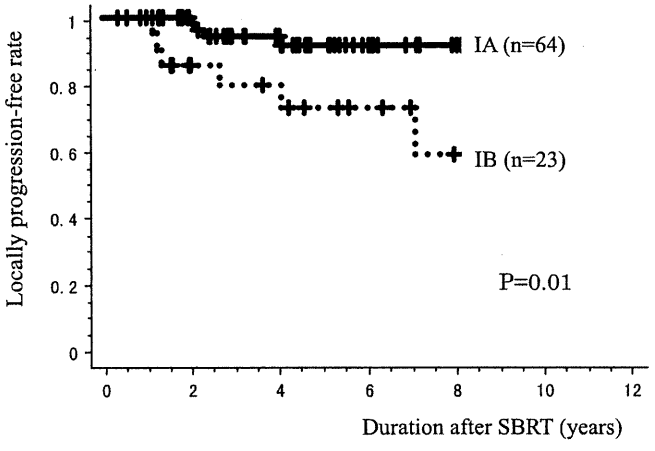

Fig. 1. Cumulative local progression–free rate curves, according to stage. SBRT = stereotactic body radiotherapy.

for the Stage IA subgroup, significantly superior ($p = 0.01$) to that for the Stage IB subgroup (73.0%; 95% CI, 52.2–93.7%). Five-year local progression–free rates were not significantly different between adenocarcinoma (80.9%; 95% CI, 68.7–93.1%) and squamous cell carcinoma (95.5%; 95% CI, 86.7–100.0%). One patient who developed local recurrence underwent surgery and has remained healthy for more than 3 years after operatively. The operation method was upper lobectomy and mediastinal lymphadenectomy, and they were performed safely without any trouble.

Cumulative curves of regional lymph node and distant metastases–free rates according to stage are shown in Figs. 2 and 3, respectively. The 5-year lymph node metastasis–free rate and distant metastasis–free rate for total cases was 85.3% (95% CI, 77.6–93.0%) and 75.1% (95% CI, 64.8–85.4%], respectively. No significant difference was identified between Stage IA and IB subgroups.

In patterns of regional nodal recurrence, 8 patients (61.5%) showed nodal failure alone, 2 patients (15.4%) had nodal failure combined with local failure, and 3 patients (23.1%) showed nodal failure combined with distant metastases.

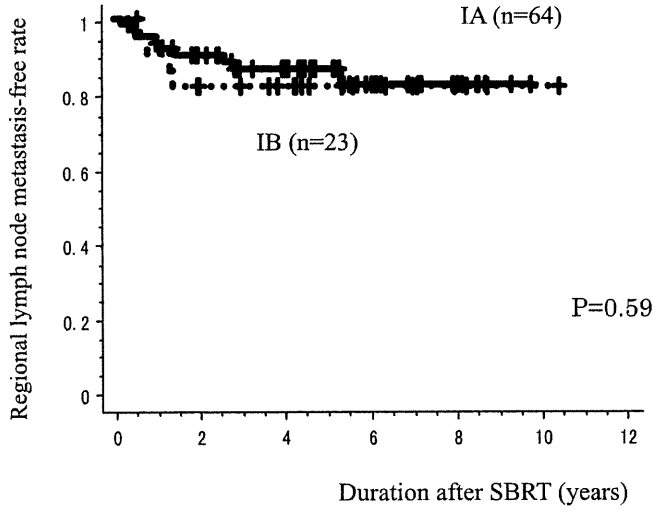

Fig. 2. Cumulative regional lymph node metastasis–free rate curves, according to stage. SBRT = stereotactic body radiotherapy.

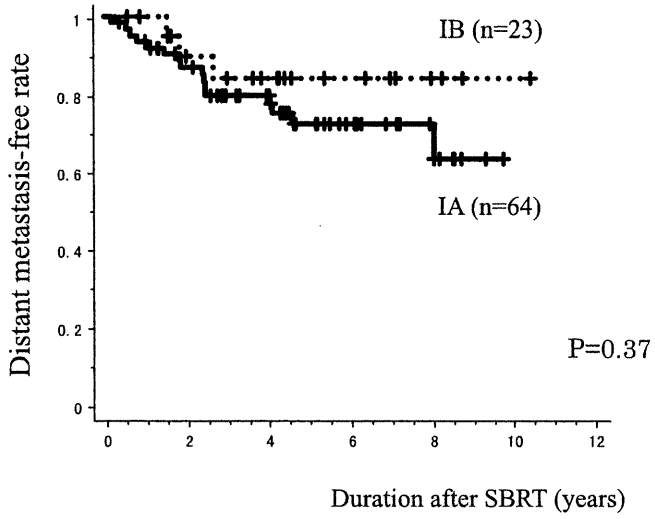

Fig. 3. Cumulative distant metastasis–free rate curves, according to stage. SBRT = stereotactic body radiotherapy.

Survival

Overall and cause-specific 5-year survival rates for total cases were 69.5% (95% CI, 58.8–80.1%) and 76.1% (95% CI, 65.9–86.3%), respectively. Overall and cause-specific survival curves according to stage are shown in Figs. 4 and 5, respectively. Five-year overall survival rate was 72.0% (95% CI, 59.6–84.4%) in Stage IA patients and 63.2% (95% CI, 42.7–83.6%) in Stage IB patients. A marginal but nonsignificant ($p = 0.14$) difference was found between overall survival rates of Stage IA and IB groups. In terms of histology, overall 5-year survival rate was 72.2% (95% CI, 59.2–85.2%) in the adenocarcinoma subgroup and 60.8% (95% CI, 38.4–83.2%) in the squamous cell carcinoma subgroup.

DISCUSSION

Exposing a tumor to a higher dose of radiation without increasing adverse effects can be achieved using stereotactic techniques. Stereotactic irradiation is an approach using

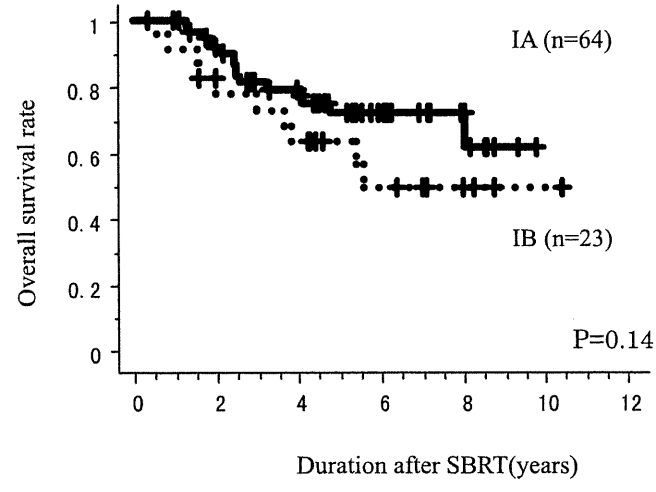

Fig. 4. Cumulative overall survival rate curves, according to stage. SBRT = stereotactic body radiotherapy.

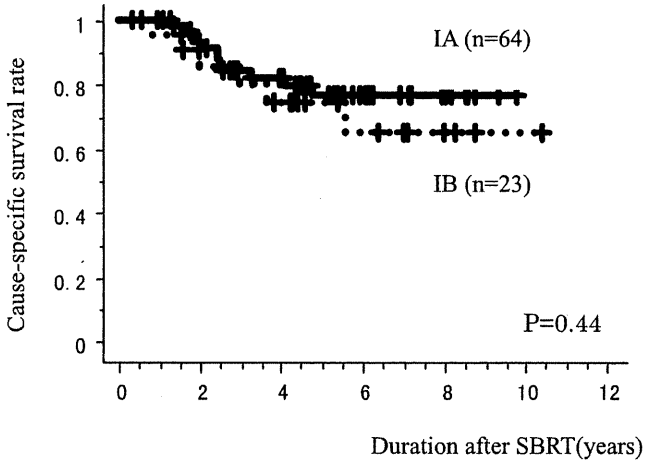

Fig. 5. Cumulative cause-specific survival rate curves, according to stage. SBRT = stereotactic body radiotherapy.

multiple noncoplanar convergent beams, precise localization with a stereotactic coordinate system, rigid immobilization, and single high-dose treatment, maximizing delivery to the tumor and minimizing the exposure of normal tissue. This approach can also substantially reduce overall treatment time from several weeks of conventional radiotherapy schedule to a few days, offering an important advantage to the patient. Stereotactic irradiation techniques are well established for the treatment of intracranial malignancies, but use in extracranial malignancies has been considered problematic because of the issues of fixation and internal motion. In 1994, Blomgren *et al.* (21) described a technique of SBRT using a custom-made body cast and stereotactic coordinates. In 1996, Uematsu *et al.* (22) reported a CT–linear accelerator unit sharing a common couch, enabling image-guided fractionated SBRT without rigid immobilization. Since verification of the effects and safety of SBRT for lung cancer (12), this treatment method has rapidly been adopted in many institutions (Table 2) (12–17, 23, 24). Although various fractionation schedules are undergoing evaluation around the world, a frequently used BED prescribed for tumors with SBRT for Stage I NSCLC in Japan has been set at a little over 100 Gy, as recommended in our previous study (18). However, concerning determination of the truly optimal dose of SBRT for Stage I NSCLC, many problems and controversies remain, such as dose-calculation algorithms (16), inhomogeneity corrections, essential dose for tumor control (24), and dose constraints for organs at risk (25, 26).

Although a number of articles on SBRT for Stage I NSCLC have been published, duration of follow-up in most cases has not been sufficiently long, and almost all treated patients were medically inoperable. The present study thus provides data on two important areas.

One was cumulative local recurrence and metastatic rates with a long duration of follow-up after SBRT. Rates of local control and metastases depend largely on the duration of follow-up and generally deteriorate as the duration of follow-up increases. Furthermore, recurrence rates have been reported in numerous articles, but most of them were crudely calculated rate. We have presented 5-year cumulative local control, regional lymph node recurrence–free and distant metastasis–free rates, calculated using Kaplan-Meier methods. The local progression–free rate in our results was unsatisfactory, particularly for the T2 tumor subgroup. The Japanese Clinical Oncology Group (JCOG) has thus started a multi-institutional dose-escalation study for Stage IB NSCLC patients (JCOG 0702).

Another meaningful result was the overall survival rate with a longer follow-up duration, allowing comparison between SBRT and surgery. Although the survival rate in this study was less than in our previous reports, we consider this information worth reporting, because median duration of follow-up was almost 5 years. Uematsu *et al.* (12) reported a 3-year overall survival rate of 86% in 29 medically operable patients with Stage I NSCLC, but the number of patients was small, and follow-up duration was relatively short. Because the number of medically operable patients treated with SBRT was very small in individual institutions, the present study collated the data of operable patients from multiple institutions. Whether the survival rate of SBRT was lower than that of surgery could not be clarified from our results. Representative 5-year overall survival rates of surgery for clinical

Table 2. Reports of SBRT for Stage I NSCLC

First author (reference)	*N*	Total dose (Gy)	Single dose (Gy)	BED (Gy)	Median follow-up (mo)	Local recurrence (%)	3-y overall survival (%)
Uematsu (12)	50	72	7.2	124	60	6*	6
Nagata (13)	42	48	12	106	52	3*	82
Onimaru (14)	28	48	12	106	27	36†	82 (Stage IA) 32 (Stage IB)
Onishi (15)	26	72	7.2	124	24	8*	75
Takeda (16)	63	50	10	100	31	5†	90 (Stage IA) 63 (Stage IB)
Koto (17)	31	45–60	7.5–15	105–113	32	29*	72
Hof (23)	10	19–26	19–26	55–94	15	40*	37
Fakiris (24)	47	60–66	20–22	180–211	50	12†	43

Abbreviations: SBRT = stereotactic body radiotherapy; NSCLC = non–small-cell lung cancer; BED = biologically effective dose ($\alpha/\beta = 10$).
* Crude data.
† Cumulative data calculated with Kaplan-Meier method.

Table 3. Comparison of 5-y overall survival rate between surgical series and SBRT

Clinical stage	United States (1)	Japanese National Cancer Center (2)	Japanese National Survey (3)	SBRT
IA	61	71	77	76
IB	40	44	60	64

Abbreviation: SBRT = stereotactic body radiotherapy.
Values are percentages.

Stage IA and IB NSCLC are listed in Table 3 (1–3), ranging approximately 60–75% for Stage IA and 40–60% for Stage IB. We cannot conclude that the survival rate for SBRT is equivalent to that for surgery, because the present data for SBRT are based on a retrospective study and small sample size. However, the background of patients treated by SBRT in this study seems likely to have included worse prognostic factors than those in patients treated surgically. Concerning the size and characteristics of tumors, good prognostic factors such as smaller tumor size (27) or lower-density mass (so-called ground-glass opacities) (28) might be more frequently included in patients treated with surgery, because the determination of histological malignancy before SBRT was difficult for such tumors. In addition, median age of patients treated by surgery was approximately 10 years younger in the surgical series (median, 60–65 years) than in the SBRT series (median, 75 years). We therefore believe that survival rates for SBRT in medically operable patients are potentially comparable to those for surgery.

Regarding treatment-related toxicity, the rate of severe (Grade ≥3) acute and short-term chronic complications after SBRT was very low and acceptable, despite the high age of those patients (median, 74 years) in our experience. In results for pulmonary lobectomy, Deslauriers *et al.* (29) reported much higher mortality and morbidity rates that increased with aging. In other reports, mortality rates for patients aged >70 years old after pulmonary lobectomy were 7.6% (30). Even though improvements of mortality and morbidity of surgery may have recently been achieved (31), in particular under a technique of video-assisted thoracoscopic lobectomy (32), we consider SBRT as a safer and less invasive treatment modality than surgery, at least for peripherally located lung tumor up to 5 years after treatment. However, reports of SBRT for centrally located lung tumor have shown a comparably high risk (25, 26), and long-term chronic toxicity remains unclear. A longer and larger follow-up of SBRT is needed.

We thus consider that SBRT may offer a useful option for initial radical treatment of at least peripheral Stage IA NSCLC, not only for medically inoperable patients but also for operable patients. However, regarding centrally located or large T2 tumors, surgery must still be recommended as the first choice of treatment until further data can be accumulated. Although we encountered only 1 case in the present study, pulmonary lobectomy and mediastinal lymph node resection were performed without difficulty for a locally recurring tumor after SBRT. Surgery might be an option as salvage therapy for locally recurrent cases after radical SBRT for Stage I NSCLC.

In Japan, the number of patients treated with SBRT has exploded, especially since SBRT for lung cancer has been covered by the national health insurance since 2004. A Phase II multi-institutional study of JCOG researching the efficacy and toxicity of SBRT for both medically operable and inoperable Stage IA NSCLC patients (JCOG 0403) started in 2004, and patient entry was completed in October 2008. A total of 90 medically inoperable and 65 operable patients have been enrolled. In the United States, a Phase II multi-institutional study of SBRT for only medically inoperable Stage I NSCLC patients (Radiation Therapy Oncology Group 0236) has been ongoing.

Even multi-institutional Phase II studies of SBRT for Stage I NSCLC may have inevitable selection bias compared with surgical series. A prospective randomized trial is essential to conclude whether outcomes of SBRT for medically operable patients are truly comparable to those of surgery. A protocol for randomized studies comparing SBRT with surgery for Stage I NSCLC has been initiated (33) but has not progressed. Such a randomized study is likely to prove very difficult to perform, because most patients may hope for more minimally invasive therapy, such as SBRT. Many more experiences for more patients with a longer follow-up duration are thus needed to confirm the safety and effects of SBRT as a radical treatment for operable Stage I NSCLC. If the experience of SBRT for medically operable Stage I NSCLC matures and produces no poor results in future, SBRT will have a marked impact on standard treatment procedures for lung cancer and provide good news for Stage I lung cancer patients, the prevalence of whom is likely to increase.

In conclusion, treatment results of SBRT reviewed from a Japanese multi-institutional database showed that SBRT is safe and promising as a radical treatment for operable Stage I NSCLC. The survival rate of SBRT is potentially comparable to that of surgery.

REFERENCES

1. Mountain CF. The international system for staging lung cancer. *Semin Surg Oncol* 2000;18:106–115.
2. Naruke T, Tsuchiua R, Kondo H, *et al.* Prognosis and survival after resection for bronchogenic carcinoma based on the 1997 TNM-staging classification: The Japanese experience. *Ann Thorac Surg* 2001;71:1759–1764.
3. Asamura H, Goya T, Koshiishi Y, *et al.* A Japanese Lung Cancer Registry study: Prognosis of 13,010 resected lung cancers. *J Thorac Oncol* 2007;3:46–52.
4. Sibley GS, Jamieson TA, Marks LB, *et al.* Radiotherapy alone for medically inoperable stage I non-small-cell lung cancer: The Duke experience. *Int J Radiat Oncol Biol Phys* 1998;40:149–154.

5. Krol AD, Aussems P, Noordijk EM, *et al.* Local irradiation alone for peripheral stage I lung cancer: Could we omit the elective regional nodal irradiation? *Int J Radiat Oncol Biol Phys* 1996;34:297–302.
6. Hayakawa K, Mitsuhashi N, Saito Y, *et al.* Limited field irradiation for medically inoperable patients with peripheral stage I non-small cell lung cancer. *Lung Cancer* 1999;26:137–142.
7. Jeremic B, Shibamoto Y, Acimovic L, *et al.* Hyperfractionated radiotherapy alone for clinical stage I nonsmall cell lung cancer. *Int J Radiat Oncol Biol Phys* 1998;38:521–525.
8. Mehta M, Scringer R, Mackie R, *et al.* A new approach to dose escalation in non-small cell lung cancer. *Int J Radiat Oncol Biol Phys* 2001;49:23–33.
9. Kong FM, Haken RK, Schipper MJ, *et al.* High-dose radiation improved local tumor control and overall survival in patients with inoperable/unresectable non-small cell lung cancer: Long-term results of a radiation dose escalation study. *Int J Radiat Oncol Biol Phys* 2005;63:324–333.
10. Narayan S, Henning GT, Haken RK, *et al.* Results following treatment to dose of 92.4 or 102.9 Gy on a phase I dose escalation study for non-small cell lung cancer. *Lung Cancer* 2004;44: 79–88.
11. Fang LC, Komaki R, Allen P. Comparison of outcomes for patients with medically inoperable Stage I non-small-cell lung cancer treated with two-dimensional vs. three-dimensional radiotherapy. *Int J Radiat Oncol Biol Phys* 2006;66:108–116.
12. Uematsu M, Shioda A, Suda A, *et al.* Computed tomography-guided frameless stereotactic radiography for stage I non-small-cell lung cancer: 5-year experience. *Int J Radiat Oncol Biol Phys* 2001;51:666–670.
13. Nagata Y, Takayama K, Matsuo Y, *et al.* Clinical outcomes of a phase I/II study of 48Gy of stereotactic body radiotherapy in 4 fractions for primary lung cancer using a stereotactic body frame. *Int J Radiat Oncol Biol Phys* 2005;63:1427–1431.
14. Onimaru R, Fujino M, Yamazaki K, *et al.* Steep dose-response relationship for stage I non-small-cell lung cancer using hypofractionated high-dose irradiation by real-time tumor-tracking radiotherapy. *Int J Radiat Oncol Biol Phys* 2008;70:374–381.
15. Onishi H, Kuriyama K, Komiyama T, *et al.* Clinical outcomes of stereotactic radiotherapy for stage I non-small cell lung cancer using a novel irradiation technique: Patient self-controlled breath-hold and beam switching using a combination of linear accelerator and CT scanner. *Lung Cancer* 2004;45:45–55.
16. Takeda A, Sanuki N, Kunieda E, *et al.* Stereotactic body radiotherapy for primary lung cancer at a dose of 50Gy total in five fractions to the periphery of the planning target volume calculated using a superposition algorithm. *Int J Radiat Oncol Biol Phys* 2009;73:442–448.
17. Koto M, Takai Y, Ogawa Y, *et al.* A phase II study on stereotactic body radiotherapy for stage I non-small cell lung cancer. *Radiother Oncol* 2007;85:429–434.
18. Onishi H, Shirato H, Nagata Y, *et al.* Hypofractionated stereotactic radiotherapy (HypoFXSRT) for stage I non-small cell lung cancer: Updated results of 257 patients in a Japanese multi-institutional study. *J Thorac Oncol* 2007;2(7 Suppl. 3): S94–S100.
19. Yaes RJ, Patel P, Maruyama Y. On using the linear-quadratic model in daily clinical practice. *Int J Radiat Oncol Biol Phys* 1991;20:1353–1362.
20. Therasse P, Arbuck SG, Eisenhauer EA, *et al.* New guidelines to evaluate the response to treatment in solid tumors. *J Natl Cancer Inst* 2000;92:205–216.
21. Blomgren H, Lax I, Naslund I, Svanstrom R. Stereotactic high dose fraction radiation therapy of extracranial tumors using an accelerator. Clinical experience of the first thirty-one patients. *Acta Oncol* 1995;34:861–870.
22. Uematsu M, Fukui T, Shioda A, *et al.* A dual computed tomography and linear accelerator unit for stereotactic radiation therapy: A new approach without cranially fixated stereotactic frame. *Int J Radiat Oncol Biol Phys* 1996;35:587–592.
23. Hof H, Herfarth KK, Munter M, *et al.* Stereotactic single-dose radiotherapy of stage I non-small-cell lung cancer (NSCLC). *Int J Radiat Oncol Biol Phys* 2003;56:335–341.
24. Fakiris AJ, McGarry RC, Yiannoutsos CT, *et al.* Stereotactic body radiation therapy forearly-stage non-small-cell lung carcinoma: four-year results of a prospective phase II study. *Int J Radiat Oncol Biol Phys* 2009;75:677–682.
25. Timmerman R, McGarry R, Yiannoutsos C, *et al.* Excessive toxicity when treating central tumors in phase II study of stereotactic body radiation therapy for medically inoperable early-stage lung cancer. *J Clin Oncol* 2006;24:4833–4849.
26. Song SY, Choi W, Shin SS, *et al.* Fractionated stereotactic body radiation therapy for medically inoperable stage I lung cancer adjacent to central large bronchus. *Lung Cancer* 2009;66:89–93.
27. Akakura N, Mori S, Okuda K, *et al.* Subcategorization of lung cancer based on tumor size and degree of visceral pleural invasion. *Ann Thorac Surg* 2008;86:1084–1091.
28. Asamura H, Suzuki K, Watanabe S, *et al.* A clinicopathological study of resected subcentimeter lung cancers: A favorable prognosis for ground glass opacity lesions. *Ann Thorac Surg* 2003; 76:1016–1022.
29. Deslauriers J, Ginsberg RJ, Dubois P, *et al.* Current operative morbidity associated with elective surgical resection for lung cancer. *Can J Surg* 1989;32:335–339.
30. Thomas P, Piraux M, Jacques LF, *et al.* Clinical patterns and trends of outcome of elderly patients with bronchogenic carcinoma. *Eur J Cardiothorac Surg* 1998;13:266–274.
31. Nagai K, Yoshida J, Nishimura M. Postoperative mortality in lung cancer patients. *Ann Thorac Cardiovasc Surg* 2007;13: 373–377.
32. Whitson BA, Groth SS, Duval SJ, *et al.* Surgery for early stage non-small cell lung cancer: A systematic review of the video-assisted thoracoscopic surgery versus thoracotomy approaches to lobectomy. *Ann Thorac Surg* 2008;86:2008–2016.
33. Hurkmans CW, Cuijpers JP, Largerwaard FJ, *et al.* Recommendations for implementing stereotactic radiotherapy in peripheral stage IA non-small cell lung cancer: Report from the Quality Assurance Working Party of the randomized phase III ROSEL study. *Radiat Oncol* 2009;4:1.

Int. J. Radiation Oncology Biol. Phys., Vol. ■, No. ■, pp. 1–8, 2011

0360-3016/$ - see front matter

ELSEVIER

doi:10.1016/j.ijrobp.2011.03.034

PHYSICS CONTRIBUTION

MEGAVOLTAGE CONE BEAM COMPUTED TOMOGRAPHY DOSE AND THE NECESSITY OF REOPTIMIZATION FOR IMAGING DOSE-INTEGRATED INTENSITY-MODULATED RADIOTHERAPY FOR PROSTATE CANCER

YUICHI AKINO, M.S.,* MASAHIKO KOIZUMI, M.D.,† IORI SUMIDA, PH.D.,*† YUTAKA TAKAHASHI, PH.D.,*† TOSHIYUKI OGATA, M.S.,*† SEIICHI OTA, B.S.,‡ FUMIAKI ISOHASHI, M.D.,* KOJI KONISHI, M.D.,* AND YASUO YOSHIOKA, M.D.*

*Department of Radiation Oncology, Osaka University Graduate School of Medicine, Suita, Osaka, Japan; †Division of Medical Physics, Oncology Center, and ‡Division of Radiology, Department of Medical Technology, Osaka University Hospital, Suita, Osaka, Japan

Purpose: Megavoltage cone beam computed tomography (MV-CBCT) dose can be integrated with the patient's prescription. Here, we investigated the effects of imaging dose and the necessity for additional optimization when using intensity-modulated radiotherapy (IMRT) to treat prostate cancer.

Methods and Materials: An arc beam mimicking MV-CBCT was generated using XiO (version 4.50; Elekta, Stockholm, Sweden). The monitor units (MU) for dose calculation were determined by conforming the calculated dose to the dose measured using an ionization chamber. IMRT treatment plans of 22 patients with prostate cancer were retrospectively analyzed. Arc beams of 3, 5, 8, and 15 MU were added to the IMRT plans, and the dose covering 95% of the planning target volume (PTV) was normalized to the prescribed dose with (reoptimization) or without optimization (compensation).

Results: PTV homogeneity and conformality changed negligibly with MV-CBCT integration. For critical organs, an imaging dose-dependent increase was observed for the mean rectal/bladder dose (D_{mean}), and reoptimization effectively suppressed the D_{mean} elevations. The bladder generalized equivalent uniform dose (gEUD) increased with imaging dose, and reoptimization suppressed the gEUD elevation when 5- to 15-MU CBCT were added, although rectal gEUD changed negligibly with any imaging dose. Whereas the dose elevation from the simple addition of the imaging dose uniformly increased rectal and bladder dose, the rectal D_{mean} increase of compensation plans was due mainly to low-dose volumes. In contrast, bladder high-dose volumes were increased by integrating the CBCT dose, and reoptimization reduced them when 5- to 15-MU CBCT were added.

Conclusion: Reoptimization is clearly beneficial for reducing dose to critical organs, elevated by addition of high-MU CBCT, especially for the bladder. For low-MU CBCT aimed at bony structure visualization, compensation is sufficient. © 2011 Elsevier Inc.

Dose compensation, Megavolt cone beam computed tomography, Prostate IMRT, Reoptimization.

INTRODUCTION

Megavoltage cone beam computed tomography (MV-CBCT) using a MV treatment beam and an electronic portal imaging device enables precise quantitative evaluation of patient setup error (1–3). The technology allows verification of organ alignment and estimation of the actual dose delivered to patients (4–6). Advantages of MV-CBCT include its stable geometry and low incidence of metal artifacts compared to kilovoltage CBCT (kV-CBCT). Disadvantages include elevated dose (7) and low image contrast compared to kV-CBCT (8), although improvements to the latter have been made (9, 10).

Intensity-modulated radiotherapy (IMRT) allows a reduction in the dose to organs at risk (OARs) by modulating the beam intensity in each beam field, using a multileaf collimator (11, 12). Pelvic organs exhibit both systematic and random motions, deformations, and size variations during treatment and over the entire course of therapy (13–16). Achieving the desired dose distribution requires still more accurate patient setup, as any uncertainty will be

Reprint requests to: Masahiko Koizumi, M.D., Ph.D., Division of Medical Physics, Oncology Center, Osaka University Hospital, 2-2(D10), Yamadaoka, Suita, Osaka, 565-0871, Japan. Tel: (+81) 6 6879 3482; Fax: (+81) 6 6879 3489; E-mail: koizumi@radonc.med.osaka-u.ac.jp

Supplementary material for this article can be found at www.redjournal.org.

Conflict of interest: none.

Acknowledgment—This work was supervised by the late Takehiro Inoue, Professor, Department of Radiation Oncology, Osaka University Graduate School of Medicine. We gratefully thank him for his wise counsel regarding the design, analysis, and reporting of this study.

Received May 11, 2010, and in revised form Feb 10, 2011. Accepted for publication March 22, 2011.

accompanied by deformation of dose distribution, resulting in the failure of dose delivery to targets and elevated dose to OARs (17). For setup verification in our institution, we routinely used a monitor unit (MU) value of 3 for CBCT, which is the minimum value for image acquisition protocols. We verified that the image quality of 3-MU CBCT was adequate for recognizing skeletal structures. For soft tissue visualization, however, we consider that 8 or more MU are required, based on clinical experience. Similarly, Morin et al. (1, 18) have suggested that the image contrast of 9-MU CBCT is sufficient for soft tissue visualization. Typically, an IMRT series consists of many fractions, and the contribution of the MV-CBCT dose may be unacceptable if image acquisition with high MU is applied to every treatment fraction. The characteristics of the CBCT beam are quite similar to those of the treatment beam, meaning that MV-CBCT dose distribution can be estimated using a radiotherapy treatment planning system (RTPS) (2). Morin et al. (18) introduced a methodology for integrating MV-CBCT dose with the prescribed dose, which used 5 MU for the head and neck region and 9 MU for the pelvic region. Those imaging doses were integrated into prescribed doses for radiotherapy by scaling down the dose weights from the total prescribed dose of the treatment beams. Miften et al. (19) showed that IMRT optimization performed after addition of the MV-CBCT beam reduced OAR dose by taking into consideration the contribution of the MV-CBCT beam. That study's MV-CBCT protocols used 15 MU for the pelvic region. The MU values for MV-CBCT were fixed in those studies, and no study has investigated the effects of MU alteration on dose distribution, although imaging dose is known to affect both patient dose and MV-CBCT image quality (2, 20).

Here, we investigated the effects of MV-CBCT imaging dose alteration and the necessity for reoptimizing MV-CBCT dose-integrated IMRT related to dose distribution in treating prostate cancer.

METHODS AND MATERIALS

Linear accelerator and MV-CBCT system

Our institution's Oncor Impression Plus linear accelerator (LINAC) with Optifocus multileaf collimator (both from Siemens Medical Solutions, Concord, CA) is capable of generating dual-energy X-ray beams (6 and 10 MV). An MVision MV-CBCT system (Siemens Medical Solutions) was installed. During MV-CBCT acquisition, the gantry of the LINAC rotates from 270° to 110°, generating a 6-MV photon beam. The field width of the MV-CBCT system is 27.4 cm. The maximum range in the superior-inferior direction is 27.4 cm, and the range can be adjusted using Y-jaws.

Dose calculation and verification of MV-CBCT accuracy

Dose distribution for MV-CBCT and treatment planning was done using an XiO version 4.50 (Elekta, Stockholm, Sweden) treatment planning system. The MV-CBCT system with doses of 3, 5, 8, and 15 MU (set MU) was calculated by regarding it as an arc beam with a gantry rotation from 270° to 110°. The calculation step of the arc beam was 10°. Field length along the Y-axis (superior-inferior direction) was 9 cm for the phantom study. The accuracy of dose calculation was verified by measurement using an I'm*RT* Phantom (IBA Dosimetry GmbH, Schwarzenbruck, Germany); a 0.6-cc Farmer-type ionization chamber, model TN30013 (PTW, Freiburg, Germany); and Gafchromic EBT2 film (International Specialty Products, Wayne, NJ).

For calculation, the I'm*RT* Phantom's electron density was considered equivalent to that of water, and the measured values were corrected using a solid phantom-to-water dose conversion factor (21). Point dose in the phantom was measured at nine points, namely the center of the phantom and points shifted vertically and horizontally by ±3 cm (Fig. 1A). To investigate the dose distribution of MV-CBCT alone, Gafchromic film in the I'm*RT* Phantom was irradiated ten times. To simulate clinical use, films were irradiated with MV-CBCT, as well as the series of IMRT beams from one patient. The summed dose distribution was analyzed. For analysis of radiochromic films, three-channel data (red-green-blue) were acquired at 150 dpi, using a flatbed scanner (model ES-10000G; Epson Seiko Corp., Nagano, Japan). We used software developed inhouse to extract red channel data from scanned images and converted them to dose distribution data, using dose calibration curve prepared for EBT2 films. We confirmed that the difference in responses of EBT2 film to 6 MV and 10 MV X-radiation was negligibly small (data not shown), and therefore, we used the calibration curve prepared using 10 MV X-rays for the analysis of films. The planar dose maps extracted from films and exported from XiO were imported into MapCHECK version 5.01.02 software (Sun Nuclear, Melbourne, FL), and the differences between dose distribution measured by films and that calculated by XiO were evaluated using the γ index (22).

Patients and IMRT planning

We retrospectively analyzed the treatment plans of 22 patients with intermediate- or high-risk prostate cancer, who were treated with IMRT between March and November 2009. A radiation oncologist delineated the prostate and seminal vesicles of all patients. The clinical target volume (CTV) was generated for the prostate and part of the seminal vesicles, and the overlapping region of the CTV with margins for all directions and rectum was then subtracted and defined as the planning target volume (PTV).

OARs were contoured by medical physicists and reviewed by a radiation oncologist. Bladder and rectal volumes were defined as solid structures within the external organ contour. The rectum was delineated from the rectosigmoid junction to the level of the ischial tuberosity or the anus. The prescribed dose was 74 Gy/37 fractions. PTV and OAR volume information for the patients is listed in Table 1. A five-field coplanar treatment plan with beam angles of 45°, 105°, 180°, 255°, and 315° was generated using a 10-MV photon beam for each patient. After optimization, the final dose was calculated using a fast Fourier transform convolution algorithm with a grid size of 2.0 mm.

Imaging dose integration and reoptimization of the IMRT plan

For all patients' IMRT plans, the dose covering 95% of PTV (D95) was normalized to the prescribed dose (74 Gy). To create simple addition plans, an arc beam mimicking 6-MV CBCT was added to the clinically approved treatment plan of each patient. The craniocaudal CBCT imaging range was 10 cm. The D95 value from total beams clearly exceeded the prescribed dose.

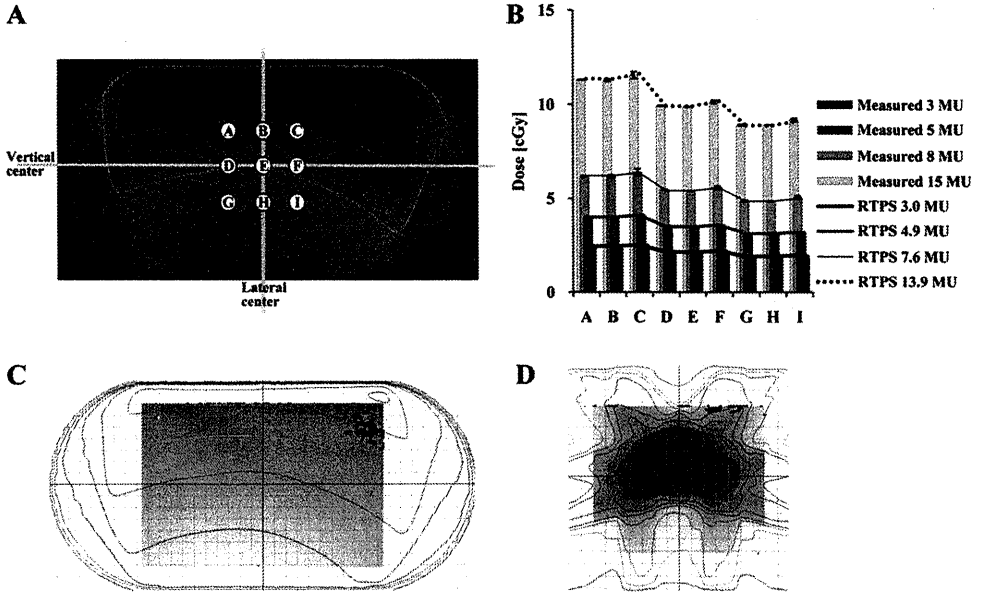

Fig. 1. (A) Dose distribution of MV-CBCT and location for measurement of point-dose using an ion chamber is shown. The axial plane of the I'm*RT* Phantom, displaying measurement points, is shown. Isodose lines show relative dose to the isocenter as calculated by using a XiO system. (B) MV-CBCT dose comparisons between measurements and calculations are shown. The horizontal axis corresponds to the location in panel A. Columns and bars represent means ± standard deviations (SDs) for measurements. The lines indicate the calculated values. The γ analysis using EBT2 film for (C) 15-MU CBCT alone and (D) IMRT beams with 3-MU CBCT of a representative patient is shown. The criterion of γ analysis is 3%/3 mm, and the region exceeding the criterion is red. The dose distributions of films and calculations are shown as gray-scale and lines, respectively.

Two further treatment plan types were created, one involving an additional round of IMRT-beam optimization (reoptimization plans) and a second without this additional optimization (compensation plans). To create compensation plans, the total dose was normalized to D95 by simple rescaling of IMRT beam weights, keeping imaging doses constant. For reoptimization plans, another optimization was performed after adding MV-CBCT. The dose constraints for reoptimization were not altered from the clinically approved treatment plans to eliminate any differences with regard to planner's individual techniques. After optimization, PTV D95 was normalized to the prescribed dose.

To assess the effects of daily portal imaging without incorporating imaging dose into the prescribed dose, two orthogonal beams mimicking portal imaging beams were created in the RTPS. The energy, field size, and imaging MU values for the portal imaging beams were 6 MV, 15 × 15 cm^2, and 1 MU, respectively, for both anterior-posterior and lateral beams. Total numbers of fractions were equal for portal imaging and IMRT. Dose calculation accuracy, linearity, and repeatability for X-ray beams with small MU were verified monthly.

Plan evaluation

To evaluate target coverage quality, PTV homogeneity (*HI*) and conformity (*CI*) indices were calculated using the following formulas:

$$HI = D_{\max}/D_{\min}$$

and

$$CI = V_{Rx}/V_{PTV}$$

where $D_{\max}$, $D_{\min}$, V_{Rx}, and V_{PTV} represent maximum dose, minimum dose, prescription isodose volume, and the PTV volume, respectively. *HI* represents the increase or decrease of hot and cold regions. The values are close to unity for homogenous plans and are large for inhomogeneous plans. *CI* stands for plan conformality. In this study, PTV D95 was normalized to the prescribed dose and was never changed by compensation and reoptimization. *CI* therefore stands for the ineffective dose delivered around PTV. *CI* values are close to unity for conformal plans and become larger for nonconformal plans.

For OARs, rectal and bladder mean doses (D_{mean}) were calculated as follows:

$$D_{mean} = \sum_i \frac{D_i V_i}{V}$$

where V_i is the volume receiving a certain dose (D_i), and V stands for total volume. To evaluate the variations of radiobiological effects from the imaging dose, the generalized equivalent uniform dose (gEUD) proposed by Niemierko (23) for each OAR was also calculated, as follows:

$$gEUD = \left(\sum_i \frac{V_i}{V} D_i^{1/n} \right)^n$$

where n is a parameter that describes the volumetric dependence of the dose-response relationship for each organ. When n = 1, the

Table 1. Patient information and calculated dose of MV-CBCT for each patients

	Volume (cc)			MV-CBCT dose (cGy)			
Dose	PTV	Rectum	Bladder	3 MU	5 MU	8 MU	15 MU
Median	71.9	42.4	132.9	80.8	131.9	204.6	374.1
Minimum	52.9	28.8	23.2	77.1	125.9	195.3	357.1
Maximum	136.9	61.3	363.0	85.4	139.6	216.5	395.9

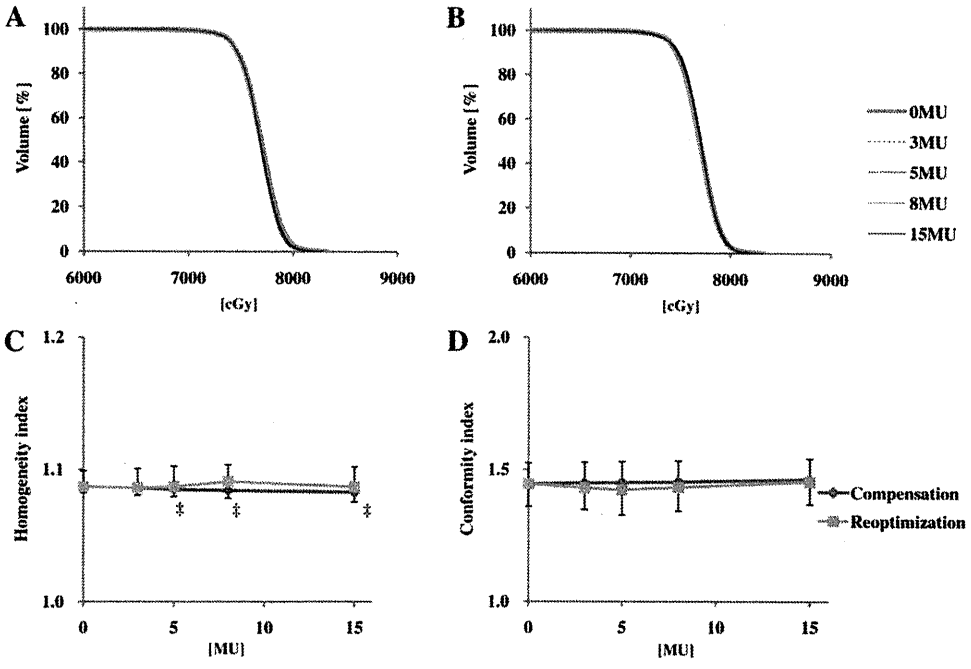

Fig. 2. Evaluation of the effects of MV-CBCT integration and reoptimization of PTV dose coverage. Representative DVHs for (A) compensation plans and (B) reoptimization plans are shown. PTV homogeneity (C) and conformity (D) indices are shown: imaging-MU is plotted along the x-axis and points and bars represent median and interquartile ranges, respectively. †, $p < 0.05$; ‡, $p < 0.01$. (Paired t-tests show a comparison between compensation and reoptimization plans with the same MU).

gEUD value is equal to D_{mean}, and a lower n value indicates stronger high-dose sensitivity. The gEUD represents the homogeneous dose distribution that results in the same probability of complications as that of an inhomogeneous dose distribution. The values of n were 0.12 and 0.5 for rectum and bladder, respectively, as Burman et al. previously reported (24). The rectal and bladder volumes receiving a certain dose (Vx) were also analyzed. For calculating D_{mean}, gEUD, and Vx, the dose-volume data were derived from dose-volume histogram (DVH) data exported from RTPS.

Statistical analyses

Statistical significance was assessed using the paired t-test, and statistical significance was set at a p value of <0.05. The Bonferroni correction was used for multiple comparison.

RESULTS

MV-CBCT dose calculation accuracy

The monitor chamber mounted on the LINAC indicated values (actual MU) of 2.7 ± 0.0, 4.5 ± 0.0, 7.2 ± 0.0, and 13.3 ± 0.1 MU for MV-CBCT beams with set MU of 3, 5, 8, and 15 MU, respectively. In a preliminary study using actual MU for calculations, unacceptable calculation errors (>10%) were observed, particularly for low-MU CBCT, although the treatment arc beam was calculated accurately (data not shown). In our study, the imaging MU values for calculations were determined by conforming the calculated dose to the dose measured using the ionization chamber. The doses from MV-CBCT for 3, 5, 8, and 15 MU (set MU) measured at the center of I'm*RT* Phantom corresponded to 3.0, 4.9, 7.6, and 13.9 MU, respectively, determined by using the XiO system. MV-CBCT doses measured by the ionization chamber and calculated by the RTPS are compared in Fig. 1B. For all eight points around the center of the I'm*RT* Phantom (Fig. 1B, point E), the error between the measured and calculated doses was less than 1.3% for all imaging MU, and the maximum absolute error was 0.08 cGy.

We also assessed MV-CBCT dose distribution calculation accuracy along the axial plane in the I'm*RT* Phantom (Fig. 1C and D). The criterion of γ analysis is 3%/3 mm, and the region exceeding the criterion was colored red. The CBCT dose distribution agreed well with the calculation (Fig. 1C). To assess the calculation accuracy for clinical use, two-dimensional dose distributions of MV-CBCT combined with IMRT beams were measured using film and compared with the calculation. The representative result using 3-MU CBCT is shown in Figure 1D. Almost all regions passed the criterion for any MU. The pass rate was greater than 98% for CBCT with or without IMRT.

Effect of reoptimization on PTV homogeneity and conformality

Figure 2A and B shows the PTV DVH for compensation and reoptimization plans, respectively. One patient with PTV and OAR volumes close to the median values was chosen. For both techniques, the curves of plans with 3- to 15-MU CBCT were highly similar to those of the nonimaging plan (0 MU), indicating little change in PTV coverage. Figure 2C and D shows PTV *HI* and *CI* indices, respectively. For *HI*, no significant differences were noted for both techniques compared with nonimaging values. Compensation with 5 to 15 MU showed a statistically significant decrease